A novel protein kinase C α-dependent signal to ERK1/2 activated by $\alpha_V\beta_3$ integrin in osteoclasts and in Chinese hamster ovary (CHO) cells

Nadia Rucci[1,*], Claudia DiGiacinto[1,*], Luigi Orrù[1], Danilo Millimaggi[1], Roland Baron[2,3] and Anna Teti[1,‡]

[1]Department of Experimental Medicine, University of L'Aquila, via Vetoio – Coppito 2, 67100, L'Aquila, Italy
[2]Department of Cell Biology and Orthopedics, Yale University School of Medicine, 333 Cedar Street, New Haven, CT 06510, USA
[3]ProSkelia SAS, 102 route de Noisy, 93230 Romainville, France

*These authors contributed equally to this work
‡Author for correspondence (e-mail: teti@univaq.it)

Accepted 11 May 2005
Journal of Cell Science 118, 3263-3275 Published by The Company of Biologists 2005
doi:10.1242/jcs.02436

Summary

We identified a novel protein kinase C (PKC)α-dependent signal to extracellular signal-regulated kinase (ERK)1/2 in mouse osteoclasts and Chinese hamster ovary (CHO) cells, specifically activated by the $\alpha_V\beta_3$ integrin. It involves translocation (i.e. activation) of PKCα from the cytosol to the membrane and/or the Triton X-100-insoluble subcellular fractions, with recruitment into a complex with $\alpha_V\beta_3$ integrin, growth factor receptor-bound protein (Grb2), focal adhesion kinase (FAK) in CHO cells and proline-rich tyrosine kinase (PYK2) in osteoclasts. Engagement of αvβ3 integrin triggered ERK1/2 phosphorylation, but the underlying molecular mechanism was surprisingly independent of the well known Shc/Ras/Raf-1 cascade, and of phosphorylated MAP/ERK kinase (MEK)1/2, so far the only recognized direct activator of ERK1/2. In contrast, PKCα was involved in ERK1/2 activation because inhibition of its activity prevented ERK1/2 phosphorylation. The tyrosine kinase c-Src also contributed to ERK1/2 activation, however, it did not interact with PKCα in the same molecular complex. The $\alpha_V\beta_3$/PKCα complex formation was fully dependent upon the intracellular calcium concentration ($[Ca^{2+}]_i$), and the use of the intracellular Ca^{2+} chelator 1,2-bis(o-amino-phenoxy)ethane-N,N,N′,N′-tetraaceticacidtetra (acetoxy-methyl) ester (BAPTA-AM) also inhibited PKCα translocation and ERK1/2 phosphorylation. Functional studies showed that $\alpha_V\beta_3$ integrin-activated PKCα was involved in cell migration and osteoclast bone resorption, but had no effect on the ability of cells to attach to LM609, suggesting a role in events downstream of $\alpha_V\beta_3$ integrin engagement.

Key words: osteoclasts, $\alpha_V\beta_3$ integrin, PKCα, c-Src, ERK1/2

Introduction

Osteoclasts are multinucleated cells, whose bone resorption function is dependent on tight, but dynamic, adhesion to the bone matrix (Boyle et al., 2003; Tanaka et al., 2003; Teitelbaum, 2000). Osteoclast adhesion structures, termed podosomes (Marchisio et al., 1984), organize the so-called actin ring, a paramarginal area that provides a tight seal to the underneath resorbing lacuna (Teti et al., 1991). Podosomes are also formed in invasive cells, such as macrophages and metastatic cancer cells, where they are called invadopodia (Chen, 1990; Kelly et al., 1994; Linder and Aepfelbacher, 2003; McNiven et al., 2004).

A substantial body of evidence suggests that the main molecular matrix-recognition mechanism of podosomes is the integrin $\alpha_V\beta_3$ (Pfaff and Jurdic, 2001; Duong et al., 2000). This integrin is predominantly expressed in cancer cells, activated endothelia and osteoclasts (Varner and Cheresh, 1996; Duong et al., 2000; Naik et al., 2003; Jin and Varner, 2004; Guo and Giancotti, 2004), and has been regarded as a potential target for controlling the abnormal behaviour of these cells in pathological conditions (Teti et al., 2002; Kumar, 2003; Nemeth et al., 2003; Jin and Varner, 2004). The integrin $\alpha_V\beta_3$ in osteoclasts recognises specific bone matrix proteins (i.e. osteopontin and bone sialoprotein II) and is activated by these ligands to provide adhesion, cytoskeletal re-organization and intracellular signalling mandatory for cell survival and bone resorbing activity (Nakamura et al., 1999; Ross et al., 1993). This receptor is expressed at high level in mature osteoclasts along with the $\alpha_2\beta_1$ receptor for type I collagen (Helfrich et al., 1996; Villanova et al., 1999).

Podosomes assemble and disassemble within minutes (Destaing et al., 2003; Saltel et al., 2004), are Ca^{2+} and pH sensitive (Teti et al., 1989; Miyauchi et al., 1990; Teti et al., 1991), and are altered by bone resorption regulating factors, which favour their assembly when resorption is stimulated. It is now well recognized that $\alpha_V\beta_3$ integrin actively participates in podosome regulation, triggering not only signal transduction pathways leading to osteoclast activation but also negative feed-back signals inducing proteasome-dependent cytoskeleton disassembly and remodelling (Sanjay et al., 2001), largely considered key events for podosome dynamisms.

It has been established that $\alpha_V\beta_3$-mediated adhesion to bone induces osteoclast extracellular signal-regulated kinase

(ERK)1/2 phosphorylation, an occurrence thought to be central to osteoclast differentiation and survival (Kim et al., 2003; Nakamura et al., 2003). The link between matrix recognition and ERK1/2 activation has not yet been fully elucidated and is likely to depend upon complex pathways. One such signal could be mediated by the serine-threonine protein kinase C (PKC), since some members of this family are known to participate in the signal cascade to ERK1/2, at least in certain circumstances (Grammer and Blenis, 1997; Aplin et al., 1998; Ni et al., 2003; Pintus et al., 2003). In osteoclasts, ERK1/2 is phosphorylated in response to calcitonin (Zhang et al., 2002), a bone resorption-inhibiting hormone that largely affects the cytoskeletal arrangement and cell motility. Interestingly, PKCs are downstream of calcitonin response (Naro et al., 1998) and regulate the phosphorylation status of proline-rich tyrosine kinase (PYK2) and focal adhesion kinase (FAK) associated with the Ca^{2+} signalling (Zhang et al., 2002). These tyrosine kinases are important integrin effectors and ERK1/2 have been reported to be activated downstream of FAK and PYK2 following integrin ligation (Chen et al., 1994). Furthermore, many of the pathways involved in cytoskeletal remodelling in osteoclasts are regulated by cytosolic Ca^{2+}. $[Ca^{2+}]_i$ increases in response to $\alpha_V\beta_3$ engagement (Duong et al., 2000), but it also causes the loss of the actin ring in a manner similar to the effect of calcitonin (Malgaroli et al., 1989; McNiven et al., 2004; Zhang et al., 2002). Cytosolic Ca^{2+} is also an effector of calcitonin response (Teti et al., 1995) and among the many roles played within the cell, it activates the Ca^{2+}-dependent members of the PKC family (Hofmann, 1997).

Taken together, these observations suggest a complex interaction among several signalling mechanisms regulating osteoclast adhesion and cytoskeletal remodelling, which could lead to assembly/disassembly cycles of podosomes and actin rings in line with the phases of bone resorption (Teti et al., 1991). We report here that PKCα isoenzyme is recruited by $\alpha_V\beta_3$ upon activation of the signal transduction pathway associated with $\alpha_V\beta_3$ and contributes to adhesion-dependent ERK1/2 activation with a novel mechanism not involving the only recognized direct ERK1/2 activator, MAP/ERK Kinase (MEK)1/2.

Materials and Methods

Materials

Cell culture media, reagents and fetal bovine serum (FBS) were from Hyclone (Röntegenstraat, The Netherlands). Culture dishes and sterile plastic ware were from Falcon Becton-Dickinson (Lincoln Park, NJ) and from Costar Co. (Cambridge, MA). The Enhanced ChemiLuminescence (ECL) kit and Hybond nitrocellulose were from Amersham Pharmacia Biotech (Little Chalfont, Bucks, UK). The anti-phospho-p44/42 ERK1/2 (cat. no. 9106), -phospho stress-activated protein kinase/c-Jun N-terminal kinase (SAPK/JNK) (cat. no. 9251), -phospho-p38 (cat. no. 9211), -MEK-1/2 (cat. no. 9122), -phospho-Src(Y416) (cat. no. 2101) were from New England Biolabs Inc. (Beverly, MA). The monoclonal anti-PKCα (cat. no. 610107), -PKCδ (cat. no. 610397) and -integrin β3 (cat. no. 61114U) were from Transduction Laboratories (Lexington, KY). The polyclonal anti-PKCα (cat. no. sc-208), -PKCβ1 (cat. no. sc-209), -PKCε (cat. no. sc-214), -PKCζ (cat. no. sc-216-G), -integrin β3 (cat. no. sc-6626), -phospho-MEK-1/2 (cat. no. sc-7995), -ERK2 (cat. no. sc-154), -JNK2 (cat. no. sc-572), -p38 (cat. no. sc-728), -PY99 (cat. no. sc-7020), -actin (cat. no. sc-1616), -focal adhesion kinase (FAK; cat. no. sc-558), -Raf-1 (cat. no. sc-133), -phospho-Raf-1 (cat. no. sc-12358), -Src-homology collagen (Shc) (cat. no. sc-1695), the monoclonal anti-Shc (cat. no. sc-967), the horseradish peroxidase (HRP)-conjugated secondary antibodies and the protein G-plus agarose (cat. no sc-2002) were from Santa Cruz Biotechnology Inc. (Heidelberg, Germany). The anti-$\alpha_V\beta_3$ (LM609), -β1 subunit (clone P5D2), -$\alpha_V\beta_5$ (clone P1F6), -$\alpha_V\beta_6$ (clone E7P6) and fluorescein isothiocyanate (FITC)-conjugated anti-mouse IgGs were from Chemicon (Temecula, CA). The anti-v-Src antibody (cat. no OP-07) was from Oncogene Research Laboratories (Boston, MA). The anti-growth factor receptor-bound protein (Grb2) antibody (cat. no 05-372), the Ras activation assay kit (cat. no 17-218), the Raf-1 kinase cascade assay kit (cat. no 17-357) and the MEK1/2 immunoprecipitation kinase assay kit (cat. no 17-159) were from Upstate (Lake Placid, NY). 1,2-bis(o-amino-phenoxy)ethane-N,N,N′,N′-tetraaceticacidtetra (acetoxymethyl) ester (BAPTA-AM) (cat. no.196419), Gö6976 (cat. no. 365250), PP2 (cat. no. 529573), 5-Iodo-3-[(3,5-dibromo-4-hydroxyphenyl)methylene]-2-indolinone (cat. no. 553008), PD98059 (cat. no. 513000) and U0126 (cat. no. 662005) were from Calbiochem (San Diego, CA). $1,25(OH)_2$vitamin D_3 was kindly provided by Domenico Criscuolo and Mauro Piatti (Roche SPA, Milan, Italy). All other chemicals, of the purest grade, were from Sigma Aldrich Chemical Co. (St Louis, MO).

Mouse bone marrow osteoclast-like cells

Differentiated primary osteoclast-like cells were obtained from the bone marrow of newborn CD1 mice by a modification of the method described by David et al. (David et al., 1998). Procedures involving animals and their care were conducted in conformity with the NIH Guide for the Care and Use of Laboratory Animals, and with our Institutional guidelines and Ethical Board provisions, in compliance of the Italian Government Regulation no. 116, 27/1/1992.

Mice were sacrificed by cervical dislocation when 5- to 7-days old, and long bones were dissected free from soft tissues and cut into small fragments. Bone marrow cells were released by gently pipetting in Dulbecco's modified minimal essential medium (DMEM) supplemented with 100 IU/ml penicillin, 100 μg/ml streptomycin, 2 mM L-glutamine and 10% FBS. Cells were plated in culture dishes and allowed to attach for 24 hours, then non-adherent cells were removed by aspiration. The total adherent cell fraction was cultured up to 7 days in the presence of 10^{-8} M $1,25(OH)_2$vitamin D_3. Osteoclast phenotype was evaluated by their multinucleate morphology and tartrate-resistant acid phosphatase (TRAcP) positivity, routinely used in this study for osteoclast recognition, as well as by resorption pit formation ability, appearance of actin rings, expression of $\alpha_V\beta_3$ integrin receptor, metalloproteinase-9 and cathepsin K and cell retraction in response to salmon calcitonin.

Chinese hamster ovary cells (CHO)

The CHO parental cells (CHOα_V) and the CHO cells stably transfected with the human β3 integrin subunit (CHO$\alpha_V\beta_3$) were kindly donated by M. H. Ginsberg and Y. Takada, Department of Vascular Biology, Scripps Research Institute, La Jolla, CA. CHOα_V cells were cultured in DMEM supplemented with antibiotics, 1% non essential amino acids and 10% FBS, at 37°C in a 95% air and 5% CO_2 incubator. CHO$\alpha_V\beta_3$ cells were cultured in the same conditions except for the culture medium which contained geneticin (700 μg/ml) for selection of transfected cells.

Adhesion assay

Tissue culture plates were coated with 10 μg/ml of LM609 in serum-free DMEM, overnight at 4°C, and blocked with 1% bovine serum albumin (BSA) in phosphate-buffer saline (PBS) for 1 hour at 37°C. Plates were fixed with 60% methanol at 4°C, washed in PBS and maintained in Tris-HCl buffer (Tris-HCl 50 mM pH 7.8, NaCl 110

mM, $CaCl_2$ 5 mM, 1% BSA, PMSF 0.1 mM) prior to use. Near confluent CHO$\alpha_V\beta_3$ cells and differentiated osteoclasts were starved overnight in DMEM containing 0.2% BSA or 1% FBS, respectively. Cells were washed in PBS and detached in 0.02% ethylene diamine tetraacetic acid (EDTA), then collected, washed in PBS, re-suspended in serum-free DMEM and held in suspension at 37°C for 1 hour. Cells were either left in suspension and collected as baseline, or placed on LM609-coated plates and allowed to adhere for various times. Cell adhesion to FBS was performed in the same conditions, with serum concentration for coating of 20% in DMEM.

To measure adhesion, CHOα_V and CHO$\alpha_V\beta_3$ cells were fixed in 80% methanol for 30 minutes, then stained with 0.5% crystal violet in 20% methanol for 5 minutes. Crystal violet was dissolved with 0.1 N sodium citrate in 50% ethanol, and absorbance, linearly proportional to the number of attached cells, was evaluated at 595 nm in an ELISA plate reader. For osteoclasts, cultures were fixed with 3.7% paraformaldehyde in 0.1 M sodium cacodylate buffer for 15 minutes and subjected to histochemical staining for TRAcP activity, using the Sigma-Aldrich kit no. 386 according to the manufacturer's instructions. The number of TRAcP-positive multinucleated cells was then counted.

Flow cytometry analysis

CHOα_V and CHO$\alpha_V\beta_3$ cells were detached at confluence by treatment with 0.02% EDTA, washed in PBS and maintained in suspension 1 hour in DMEM plus 10% FBS and 1% nonessential amino acids. Cells were then incubated with 10 μg/ml of primary antibody for 1 hour at 4°C, washed in PBS and incubated with FITC-labelled secondary antibody for 1 hour at 4°C. After washing in PBS, cell surface immunofluorescence was analysed by a flow cytometer fluorescence-activated cell sorting (FACS)scan (Becton Dickinson, Mountain View, CA).

Total protein extraction and immunoprecipitations

Cells adherent to LM609 or in suspension were washed in PBS and lysed in RIPA buffer (10 mM Tris-HCl pH 7.2, 1% Nonidet P-40, 158 mM NaCl, 1 mM EDTA, 50 mM NaF, 1 mM PMSF, 10 μg/ml aprotinin, 10 μg/ml leupeptin, 1 mM sodium orthovanadate, 10 mM sodium pyrophosphate). Protein content was measured by the Bradford method. For immunoprecipitations, 5 μg of specific antibodies with or without preimmune serum were incubated for 2 hours at 4°C with protein G-conjugated agarose beads. After five washes in RIPA buffer, 1 mg of each sample was added and incubated with beads overnight at 4°C. Samples were then washed five times with RIPA buffer, re-suspended in 2× reducing or nonreducing Laemmli sample buffer and boiled prior to SDS-PAGE.

Cell protein fractionation

Cells adherent to LM609 or maintained in suspension were lysed in hypotonic homogenization buffer (10 mM Tris-HCl pH 7.4, 0.5 mM EDTA, 1 mM sodium orthovanadate, 1 mM PMSF, 10 μg/ml aprotinin, 10 μg/ml leupeptin) for 20 minutes on ice after washing with PBS and centrifuged at 30,000 ***g*** for 30 minutes at 4°C. The soluble cytosolic fraction was recovered while the pellets were solubilized in homogenization buffer containing 1% Triton X-100. The soluble membrane fraction was then recovered after centrifugation at 30,000 ***g*** for 30 minutes at 4°C. The Triton X-100-insoluble pellets were re-suspended in RIPA buffer and supernatants (Triton X-insoluble fraction) were collected after centrifugation at 10,000 ***g*** for 30 minutes at 4°C.

For cytosol and nuclear protein extraction, cells were homogenized in Yoshi A buffer (10 mM Tris-HCl pH 8, 1.5 mM $MgCl_2$, 10 mM KCl) plus protease inhibitors and centrifuged at 720 ***g*** for 10 minutes at 4°C. Supernatants (cytosol fraction) were collected, centrifuged at 11,600 ***g*** for 20 minutes a 4°C. Pellets of the first centrifugation were resuspended in Yoshi B buffer (20 mM Tris-HCl pH 8, 25% glycerol, 0.42 mM NaCl, 1.5 mM $MgCl_2$, 0.2 mM EDTA) plus protease inhibitors, and supernatants (nuclear fraction) were collected after centrifugation at 11,600 ***g*** for 20 minutes at 4°C.

Protein content was determined in each fraction by the Bradford method.

Western blotting

Immunoprecipitation samples, 30-60 μg of total proteins or 30 μg of fractionated proteins, were subjected to 10% SDS-PAGE, then electro-transferred to nitrocellulose membranes. After blocking of blots with 5% non-fat milk in TBS-T buffer (20 mM Tris-HCl, pH 7.6, 137 mM NaCl, 0.2% Tween 20), specific primary antibodies, diluted in 1% non-fat milk in TBS-T as indicated in figure legends, were incubated with the blots at 4°C, overnight. Species-specific HRP-conjugated secondary antibodies were diluted 1:5,000 in 1% non-fat milk in TBS-T and incubated for 1 hour at room temperature prior to ECL detection of immuno-complexes, according to the manufacturer's instructions.

GTP-Ras detection assay

GTP-Ras was detected by the Upstate Ras activation assay kit according to the manufacturer's instructions. Briefly, cells were collected and homogenized in 1× MLB Buffer (Mg^{2+} lysis/wash buffer). Cell lysates were centrifuged (5 minutes, 10,000 ***g***, 4°C), then supernatants containing the protein fraction were recovered and incubated with Raf-1 RBD (Ras assay reagent) agarose for 45 minutes at 4°C under gentle agitation. Samples were then centrifuged and the agarose beads washed three times with 1× MLB and resuspended in 2× Laemmli reducing sample buffer. After boiling, samples were subjected to 10% SDS-PAGE, then electro-transferred to nitrocellulose membranes. After blocking with 5% non-fat milk in TBS-T buffer, filters were incubated overnight at 4°C with anti-Ras antibody (1 μg/ml) in TBS-T plus 1% non-fat milk, washed three times and incubated with HRP-conjugated secondary antibody (dilution 1:5,000). The immunoreaction was detected by ECL.

Raf-1 and MEK1/2 kinase assays

Raf-1 and MEK1/2 kinase assays were performed using the Upstate Raf-1 kinase cascade assay kit and MEK1/2 immunoprecipitation kinase assay kit according to the manufacturer's instructions. Briefly, cell lysates were incubated with inactive MEK1/2 substrate (Raf-1 kinase assay) or inactive MAP kinase 2/Erk 2 substrate (MEK1/2 kinase assay), and with the magnesium/ATP cocktail for 30 minutes at 30°C under gentle agitation. Samples were then centrifuged and incubated with myelin basic protein and [γ-^{32}P]ATP for 10 minutes at 30°C under agitation. At the end of the incubation, samples were transferred to phosphocellulose squares, washed three times with 0.75% phosphoric acid and once with acetone, then the incorporated radioactivity was counted using a β-counter.

CHO$\alpha_V\beta_3$ migration and invasion assays

For migration assay, CHO$\alpha_V\beta_3$ cells were pretreated with 6 nM Gö6976 for 30 minutes, then plated in the upper compartment of a transwell chamber on 12 μm polycarbonate filters pre-coated with 10 μg/ml LM609. After 4 hours of incubation in the presence of NIH3T3-cell-conditioned medium, added to the lower compartment as chemoattractant, filters were stained with Hematoxylin/Eosin. Cell migration ability was evaluated by counting the cells migrated to the lower side of the filters in five randomly chosen fields.

Invasion assay was performed with the same protocol, except that filters were pre-coated with 15 μg/cm^2 Matrigel.

Osteoclast migration assay

Osteoclasts were detached in 0.02% EDTA, pretreated with 2 μM Gö6976 for 30 minutes, then plated in the upper compartment of a transwell chamber on 12 μm polycarbonate filters pre-coated with 10 μg/ml LM609 (Chellaiah et al., 2000). After 12 hours in the presence of 25 μg/ml osteopontin added to the lower compartment as chemoattractant, filters were stained for TRAcP and osteoclast migration evaluated by counting the cells migrated to the lower side of the filters in five randomly chosen fields.

Bone resorption

Osteoclasts were detached in 0.02% EDTA, pre-treated with 2 μM Gö6976 for 30 minutes and re-plated on bone slices in the presence of the inhibitor for 48 hours. Bone slices were then fixed in 3% paraformaldehyde in 0.1 M cacodylate buffer, cells were removed by ultrasonication in 1% sodium hypochlorite, and slices were stained with 0.1% Toluidine Blue. Pits were counted and the pit index computed according to the method of Caselli et al. (Caselli et al., 1997).

Statistical analysis

Quantitative data are expressed as the mean ± s.e.m. of at least three independent experiments. Statistical analysis was performed using one-way analysis of variance (ANOVA), followed by the unpaired Student's *t*-test. A P value <0.05 was considered statistically significant.

Results

Integrin profile and adhesion to LM609

The aim of this study being to delineate the role of PKC family members in $\alpha_V\beta_3$ integrin-mediated signalling, we used as a substrate immobilized LM609, a monoclonal antibody specifically recognizing this integrin. Fig. 1A shows the integrin profile of parental CHO cells, expressing the α_V but not the β_3 subunit (CHOαV), and CHO cells stably transfected with the β_3 subunit (CHO$\alpha_V\beta_3$). When expressed (Fig. 1Aa), the exogenous β_3 subunit functionally associated with the α_V to form the $\alpha_V\beta_3$ receptor (Fig. 1Ab lower left panel). CHO$\alpha_V\beta_3$ cells adhered to LM609 more slowly than to FBS, but after 60 minutes the number of attached cells was indistinguishable between the two substrates (Fig. 1B, lower panels). In contrast, the β3-negative CHOα_V cells, which adhered to FBS in a manner similar to CHO$\alpha_V\beta_3$ cells, failed to recognise the immobilized LM609 and their adhesion to this substrate was negligible at any time tested (Fig. 1B, upper panels).

In similar assays, prompt adhesion of multinucleated osteoclasts and their putative TRAcP-positive mononuclear precursors to immobilized LM609 was observed, with a kinetics analogous to that of adhesion to FBS-coated substrate, but slower than that of CHO$\alpha_V\beta_3$ cells (Fig. 1C).

PKC activation and subcellular redistribution

To test whether specific PKC isoforms were engaged in the signalling pathways triggered by $\alpha_V\beta_3$ integrin, we performed western blot analysis of fractionated cell lysates, which were then probed with antibodies against members of all classes of PKCs. We noted that in CHO$\alpha_V\beta_3$ cells, adhesion to LM609 induced time-dependent translocation of the classical PKCα

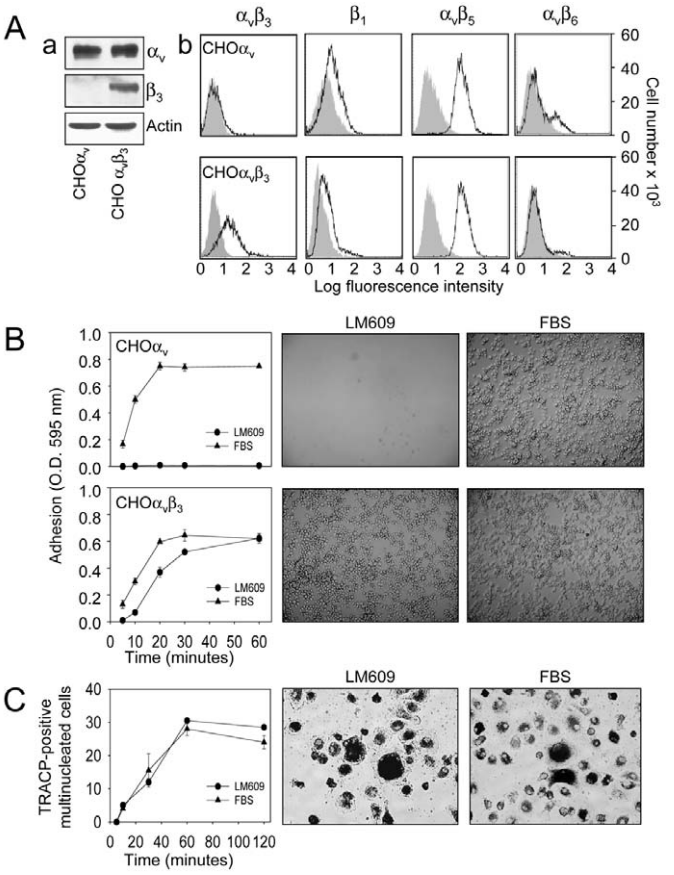

Fig. 1. Integrin expression profile and adhesion to LM609. (A) Parental CHO cells (CHOα_V) and clonal CHO$\alpha_V\beta_3$ cells were subjected to (a) western blot analysis for α_V and β_3 subunits (primary antibodies diluted 1:300), and (b) to FACS analysis for $\alpha_V\beta_3$, β_1, $\alpha_V\beta_5$ and $\alpha_V\beta_6$ integrin expression profile. Grey shadows, fluorescence background; black traces, integrin-specific fluorescence intensity. (B) CHOα_V and CHO$\alpha_V\beta_3$ cells were allowed to adhere to immobilized LM609 monoclonal antibody or FBS for the time indicated in graphs (left panels, crystal violet staining), or for 30 minutes for morphological analysis (middle and right panels, phase contrast microscopy). Original magnification 10×. (C) Osteoclast cultures (including TRAcP-positive mature multinucleated cells and putative mononuclear precursors) were obtained from bone marrow as described in Materials and Methods, gently lifted in 0.02% EDTA-containing buffer and allowed to attach to immobilized LM609 or FBS for the time indicated in graph (left panel) or for 30 minutes for morphological analysis (middle and right panels, staining for TRAcP). Original magnification 20×.

from the cytosol to the membrane and to the Triton X-100-insoluble compartments (Fig. 2A, first row). Translocation was apparent after 5 minutes of adhesion, peaking at 20 minutes and remaining stable thereafter. In the same circumstance, translocation of classical PKCβ1 was also noticed. Already after 5 minutes, translocated PKCβ1 appeared in the Triton X-100-insoluble fraction followed by its appearance in the membrane fraction after 10 minutes. It then increased with time only in the former compartment disappearing from the latter at 30 minutes (Fig. 2A, second row). This cellular redistribution of classical PKCs was assumed to be consistent with activation of their catalytic function as it was also induced

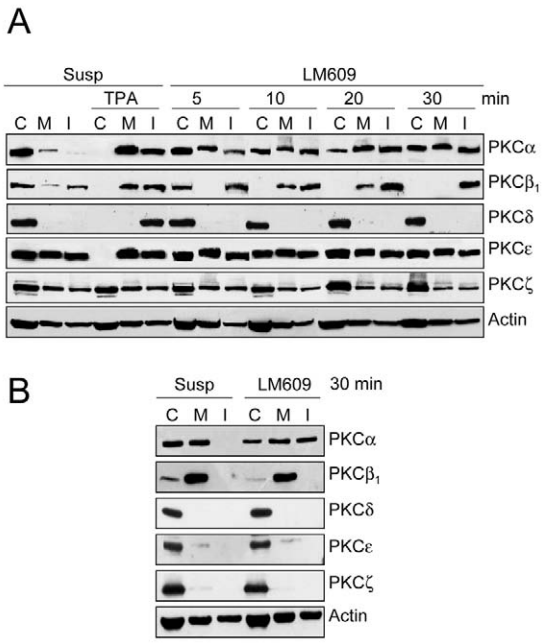

Fig. 2. PKC isoform expression and subcellular redistribution. (A) CHO$\alpha_V\beta_3$ cells were serum-starved, detached and kept in suspension for 1 hour, then replated in LM609-coated wells for the indicated times. Aliquots of cells were left untreated (suspension) for baseline detection, or treated with 10^{-7} TPA for 5 minutes to activate classical and novel PKCs. Cell proteins were fractionated as described in Materials and Methods, resolved by SDS-PAGE and western blotted with the indicated anti-PKC (diluted 1:800), or with anti-actin (diluted 1:1000) antibodies for normalization. (B) Osteoclasts were lifted, replated in LM609-coated wells for 30 minutes and processed for PKC or actin detection as described in A. C, cytosolic; M, membrane; I, Triton-X-100-insoluble fractions; Susp, cells in suspension; LM609, adhesion to LM609 for 30 minutes. Similar results were obtained in three independent experiments.

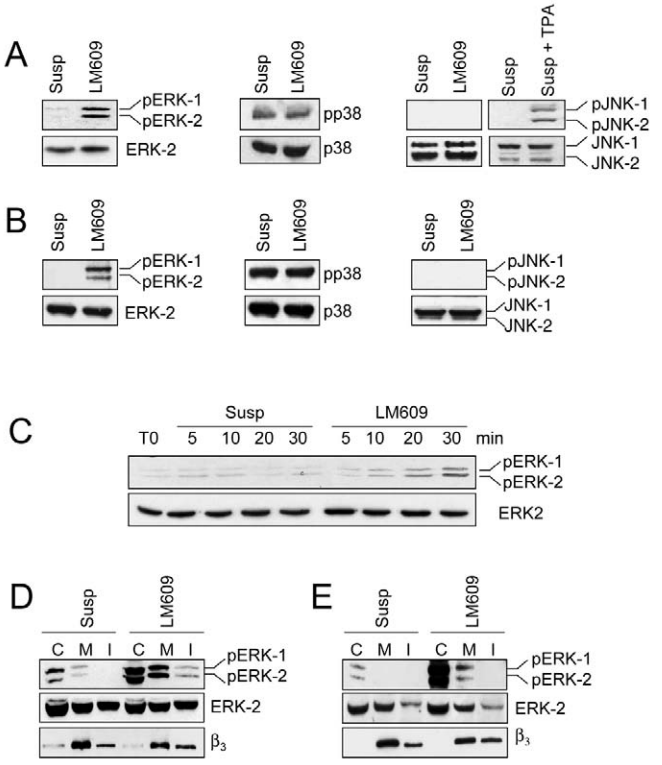

Fig. 3. Detection of total and phosphorylated MAPKs. (A) CHO$\alpha_V\beta_3$ cells and (B) osteoclast cultures were prepared as described in Fig. 2 and plated in LM609-coated wells for 30 minutes. An aliquot of suspended cells was also treated for 5 minutes with TPA (10^{-7} M) to show control positive assay for phosphorylated JNK. Total cell lysates were processed by SDS-PAGE and western blot for detection of total and phosphorylated fractions of ERK1/2 (primary antibodies diluted 1:500), p38 (primary antibodies diluted 1:800) and JNK (primary antibodies diluted 1:500). (C) Aliquots of CHO$\alpha_V\beta_3$ cells were maintained in suspension or plated in LM609-coated wells for the indicated times, with T0 representing cells cultured in standard conditions, starved overnight in serum-free medium. Cells were processed as described above and total and phosphorylated ERK1/2 were determined. (D) Fractionated CHO$\alpha_V\beta_3$ cell and (E) osteoclast lysates, obtained as described in Fig. 2, were probed with anti-total or anti-phosphorylated ERK, and anti-β_3 integrin antibodies (diluted 1:400) C, cytosolic; M, membrane; I, Triton-X-100-insoluble fractions; Susp, cells in suspension; LM609, adhesion to LM609 for 30 minutes. Similar results were obtained in three independent experiments.

by short-term (5 minutes) treatment with 12-O-tetradecanoylphorbol-13-acetate (TPA) (Fig. 2A, first and second rows), a reagent known to activate classical and novel PKCs within minutes of exposure (Housey et al., 1988). In contrast, members of the novel (PKCδ, PKCε) and atypical (PKCζ) subfamilies were not affected by adhesion of CHO$\alpha_V\beta_3$ cells to LM609. As expected, the former PKCs were then again activated by TPA within 5 minutes of treatment (Fig. 2A, third and fourth rows).

Similar to CHO$\alpha_V\beta_3$ cells, osteoclasts attached to LM609 also showed cellular redistribution of PKCα unlike osteoclasts kept in suspension. In these cells, however, the PKCα isoenzyme was already abundant in the membrane in suspended cells and was then mainly recruited to the Triton X-100-insoluble fraction upon adhesion to substrate (Fig. 2B, first row). In contrast, PKCβ1 did not appear to be affected by $\alpha_V\beta_3$ integrin-mediated adhesion of osteoclasts, as it remained in the cytosolic and membrane compartments (Fig. 2B, second row). Similar to CHO$\alpha_V\beta_3$ cells, members of the novel (PKCδ and PKCε) and atypical (PKCζ) classes remained unaffected upon adhesion to LM609 (Fig. 2B, third to fifth rows). Thus, engagement of $\alpha_V\beta_3$ integrin in CHO$\alpha_V\beta_3$ cells and osteoclasts lead to the translocation and activation of classical, but not novel and atypical, PKCs.

MAPK phosphorylation

Since MAPK are activated downstream of $\alpha_V\beta_3$ and PKCs, we then assessed changes in the MAPK activation profile. Cells were allowed to attach to LM609 for 30 minutes and evaluated by western blot using antibodies recognizing the phosphorylated forms of ERK1/2, p38 and JNK. In both CHO$\alpha_V\beta_3$ cells (Fig. 3A) and osteoclasts (Fig. 3B), increase in the phosphorylated species of ERK1/2 was observed upon adhesion to LM609 (Figs 3A,B left panels). In contrast, phospho-p38 remained unchanged and phospho-JNK was

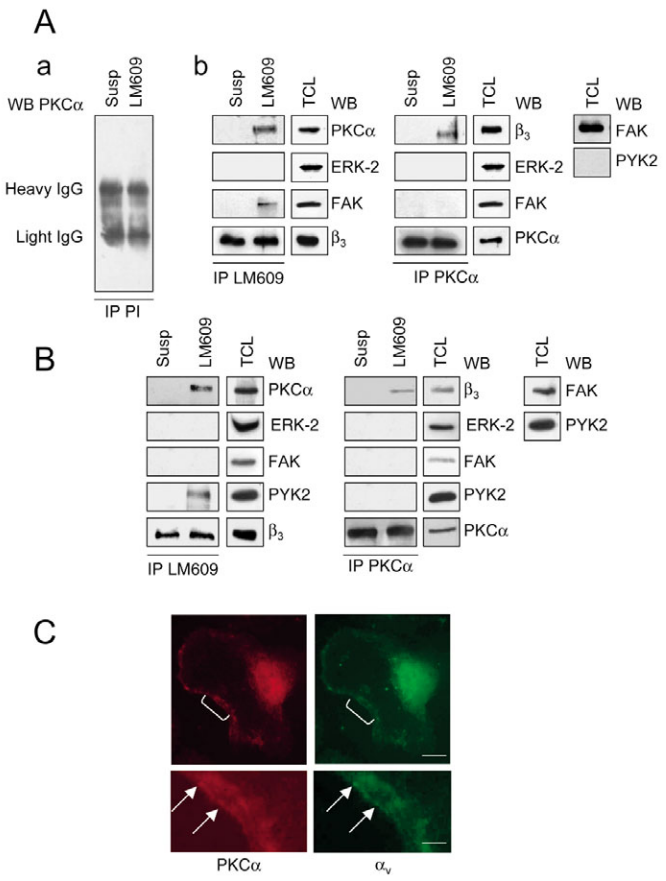

Fig. 4. Immunoprecipitation assays. (A) CHO$\alpha_V\beta_3$ cells and (B) osteoclast cultures were treated as described in Fig. 2, immunoprecipitated with the indicated antibodies and western blotted for PKCα (diluted 1:800), FAK (diluted 1:1000), PYK2 (diluted 1:500), ERK-2 and β_3 detection (left and middle panels). Total cell lysates were also subjected to SDS-PAGE and western blotted for total FAK and PYK2 detection in CHO$\alpha_V\beta_3$ cells (A, right panels) and osteoclasts (B, right panels). Similar results were obtained in three independent preparations. IP, immunoprecipitation; PI, preimmune serum; TCL, total cell lysate; WB, western blot analysis; Susp, cells in suspension; LM609, adhesion to LM609 for 30 minutes. (C) An osteoclast plated in an LM609-coated well was immunostained with anti-PKCα (diluted 1:10) and α_V (diluted 1:10) antibodies detected by conventional immunofluorescence using TRITC- (diluted 1:200) and FITC- (diluted 1:160) conjugated secondary antibody, respectively. Note that the osteoclast was allowed to adhere for 30 minutes, a time insufficient to permit actin ring formation. Scale bars: 20 μm (upper panels); 5 μm (lower panels). Brackets in the upper panels delineate the area showed at higher magnification in the lower panels. Arrows indicate areas of overlapping red (PKCα) and green (α_V) fluorescent labels.

undetectable both in suspended cells and in cells attached to LM609 (Fig. 3A,B middle and right panels, respectively). Fig. 3A also includes a phospho-JNK-positive control obtained by treating CHO$\alpha_V\beta_3$ cells with 10^{-7} TPA for 5 minutes.

In CHO$\alpha_V\beta_3$ cells, ERK1/2 phosphorylation was clearly appreciable after 10 minutes of adhesion, and increased with time up to 30 minutes (Fig. 3C). Analysis of fractionated CHO$\alpha_V\beta_3$ cells (Fig. 3D) and osteoclasts (Fig. 3E) showed that total ERK1/2 was distributed in the cytosol, membrane and Triton X-100-insoluble fractions, and that adhesion to LM609 triggered its phosphorylation mostly in the cytosol and membrane compartments, with little, if any, activation in the Triton X-100-insoluble fraction.

$\alpha_V\beta_3$/PKCα complex

Immunoprecipitations with preimmune serum (Fig. 4Aa) demonstrate absence of non-specific bands in the assays (shown here for PKCα, not shown for all other assays). To assess whether PKCα was recruited in a complex with the $\alpha_V\beta_3$ integrin, lysates from suspended and adherent cells were immunoprecipitated with LM609 antibody and western blotted with anti-PKCα antibody. Adhesion to immobilized LM609 recruited PKCα in a complex with $\alpha_V\beta_3$ integrin both in CHO$\alpha_V\beta_3$ cells and osteoclasts (Fig. 4Ab,B, left panels). Reciprocal immunoprecipitation of the same lysates with anti-PKCα antibody confirmed co-immunoprecipitation in the same complex of both PKCα and $\alpha_V\beta_3$ integrin (Fig. 4Ab,B, middle panels). This complex did not appear to recruit ERK, suggesting that this MAPK could be phosphorylated upon $\alpha_V\beta_3$ engagement only downstream and not by direct association. The complex recruited FAK in CHO$\alpha_V\beta_3$ cells and PYK2 in osteoclasts (Fig. 4Ab,B, left panels). This difference was not surprising as FAK was the only species expressed by CHO$\alpha_V\beta_3$ cells (Fig. 4Ab, right panels), and PYK2 was the major species expressed by osteoclasts (Fig. 4B, right panels). However, immunoprecipitation with PKCα antibody failed to reveal co-precipitated FAK or PYK2 (Fig. 4Ab,B middle panels), suggesting that these adhesion tyrosine kinases could interact only with the $\alpha_V\beta_3$ integrin and not with PKCα. Fig. 4C, shows immunofluorescence analysis of an osteoclast attached to LM609 for 30 minutes, where PKCα (left panels) and α_V integrin subunit (right panels) appear to localize in the same paramarginal area.

At variance with PKCα, activated PKCβ1 failed to associate with the $\alpha_V\beta_3$ receptor in CHO$\alpha_V\beta_3$ cells (not shown), suggesting that its recruitment to the Triton X-100-insoluble fraction observed in this cell type does not require direct interaction with the integrin.

ERK1/2 activation pathway

ERK activation in response to $\alpha_V\beta_3$ integrin engagement could be dependent upon activation of the Ras pathway. Indeed it has been proposed that integrin-dependent Ras activation is a consequence of the engagement of the Shc/Grb2 complex (Foschi et al., 1997). To address whether $\alpha_V\beta_3$ integrin requires this molecular interaction to trigger ERK1/2 phosphorylation, we tested whether Shc was recruited in a complex with $\alpha_V\beta_3$ upon adhesion to LM609. Our results failed to demonstrate an $\alpha_V\beta_3$/Shc complex in either CHO$\alpha_V\beta_3$ cells (Fig. 5A, left panels) or osteoclasts (Fig. 5B, left panels) attached to LM609. Consistently, in PKCα antibody immunoprecipitates from the same lysates, Shc was not apparent upon adhesion to LM609 (Fig. 5A,B, middle panels). In addition, no changes in Shc subcellular distribution (not shown) or in its phosphorylation status (Fig. 5A,B, right panels) were observed in both cell types attached to LM609, relative to suspended cells.

In contrast to Shc, Grb2, which is also known to be activated by direct binding to FAK or PYK2 through its SH2 domain

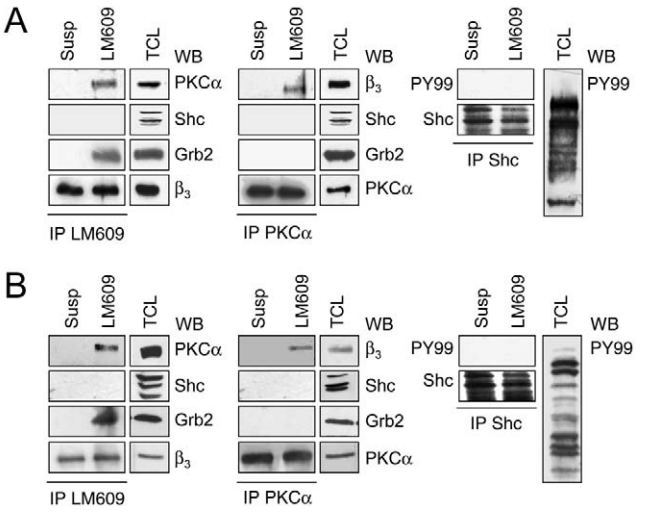

Fig. 5. Recruitment of Shc and Grb2. (A) CHO$\alpha_V\beta_3$ cells and (B) osteoclast cultures were treated as described in Fig. 2, immunoprecipitated with the indicated antibodies and western blotted to detect PKCα, Shc (diluted 1:200), Grb2 (diluted 1:1000) and β_3 integrin (left and middle panels), or to detect total tyrosine-phosphorylated proteins using the PY99 (diluted 1:1000) antibody (right panels). Similar results were obtained in three independent experiments. IP, immunoprecipitation; TCL, total cell lysate; WB, western blot analysis; Susp, cells in suspension. LM609, adhesion to LM609 for 30 minutes.

independent of the Shc adaptor protein (Schlaepfer et al., 1994), was recruited by the integrin upon adhesion to LM609 (Fig. 5A,B left panels). It could not, however, be detected in PKCα immunoprecipitates either in CHO$\alpha_V\beta_3$ cells (Fig. 5A middle panels), or in osteoclasts (Fig. 5B middle panels), suggesting no physical interaction with the kinase.

To address whether Ras was activated by adhesion to LM609, CHO$\alpha_V\beta_3$ cells and osteoclasts were allowed to attach for 30 minutes and Ras activity evaluated by the appearance of GTP-Ras. Consistent with the previous results, GTP-Ras was not found to be increased by adhesion to LM609 in CHO$\alpha_V\beta_3$ cells (Fig. 6A). An analogous negative result was observed when Raf-1 activation was evaluated in immobilized LM609-attached cells. In fact, immunoprecipitated Raf-1 was not serine- (Fig. 6B) or tyrosine- (Fig. 6C) phosphorylated upon substrate recognition. Consistent with these results, immunoprecipitated Raf-1 failed to recruit PKCα (Fig. 6B) as well as c-Src (Fig. 6C), which is implicated in the tyrosine phosphorylation required for its full activation. Positive controls, performed by treatment of serum-starved cells with 20% FBS, showed integrity of these pathways, with expected PKCα recruitment and Raf-1 serine phosphorylation (Fig. 6B) as well as c-Src recruitment and Raf-1 tyrosine phosphorylation (Fig. 6C) in Raf-1 immunoprecipitates. Furthermore, treatment with 15 μM Raf-1 inhibitor, 5-iodo-3-[(3,5-dibromo-4-hydroxyphenyl)methylene]-2-indolinone, was without effect on CHO$\alpha_V\beta_3$ cells attached to LM609 (Fig. 6D, right panels), while blocking ERK1/2 activation in FBS-treated cells (Fig. 6D, left panels). Finally, Raf-1 kinase assay demonstrated no activity of the kinase in response to adhesion to LM609, as opposed to treatment with FBS (Fig. 6F).

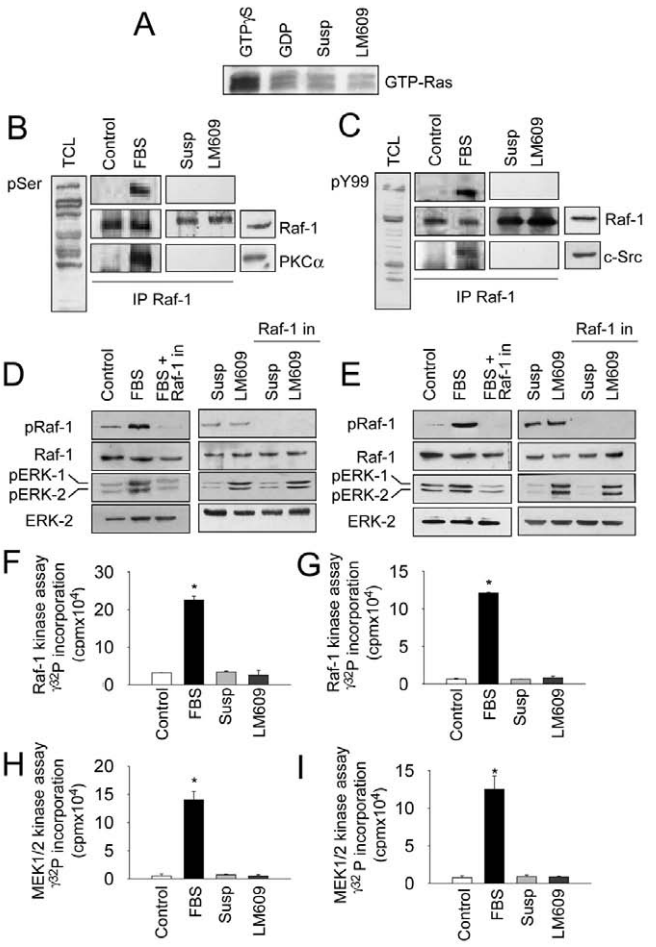

Fig. 6. Ras/Raf-1/MEK1/2 activation. CHO$\alpha_V\beta_3$ cells were treated as described in Fig. 2 and probed for detection of (A) GTP-Ras (diluted 1:800), (B) serine- (diluted 1:500; left panels) and (C) tyrosine- (diluted 1:1000; right panels) phosphorylated Raf-1, co-precipitated PKCα (left panels) and c-Src (right panels). An aliquot of cells in standard culture conditions was serum-starved overnight, then treated with 20% FBS for 30 minutes to show the integrity of the Raf-1 pathway (B,C). In A, the GTP analogue, GTPγS, and GDP were added in the assay for positive and negative control, respectively. (D) CHO$\alpha_V\beta_3$ and (E) osteoclasts were treated as described above in the presence of the Raf-1 inhibitor 5-iodo-3-[(3,5-dibromo-4-hydroxyphenyl)methylene]-2-indolinone (Raf-1 in; 15 μM, 30 minutes) prior to treatment with 20% FBS or plating on LM609-coated wells for 30 minutes. Cells were then processed for SDS-PAGE and western blot for detection of total and phosphorylated Raf-1 and ERK1/2. (F) CHO$\alpha_V\beta_3$ cells and (G) osteoclasts were treated as above but in the absence of the inhibitor, lysed and tested for Raf-1 kinase activity using the Upstate Raf-1 kinase cascade assay kit. (H,I) Lysates from (H) CHO$\alpha_V\beta_3$ cells and (I) osteoclasts were also tested using the MEK1/2 immunoprecipitation kinase assay kit for detection of MEK1/2 kinase activity. Similar results were obtained in three independent experiments. IP, immunoprecipitation; TCL, total cell lysate; WB, western blot analysis; Susp, cells in suspension; LM609, adhesion to LM609 for 30 minutes. For F-I results are the mean ± s.e.m. of three independent experiments, with $^*P<0.0001$.

Similar independence of this pathway was observed in osteoclasts, as suggested by lack of both appearance of GTP-

Ras, and Raf-1 serine and tyrosine phosphorylation (not shown). Furthermore, no changes in ERK1/2 activation in the presence of the Raf-1 inhibitor (Fig. 6E), or Raf-1 kinase activity (Fig. 6G) were observed in osteoclasts attached to LM609 as opposed to FBS-treated osteoclasts.

We then assessed the involvement of MEK1/2 in $\alpha_V\beta_3$-mediated intracellular signalling. MEK1/2 kinase assays showed intense activity in response to treatment with FBS, but failed to demonstrate any detectable change over baseline in response to adhesion to LM609 both in CHO$\alpha_V\beta_3$ cells (Fig. 6H) and in osteoclasts (Fig. 6I). Furthermore, CHO$\alpha_V\beta_3$ cells (Fig. 7A,B) and osteoclasts (Fig. 7C) attached to LM609 failed to show increased MEK1/2 phosphorylation. Treatments with the MEK1/2-specific inhibitors PD98059 and U0126 proved efficacious in inhibiting MEK1/2 phosphorylation in both CHO$\alpha_V\beta_3$ cells (Fig. 7B, upper panels) and osteoclasts (Fig. 7C, upper panels). However, in this circumstance, consistent with the previous results, no effect on adhesion-induced ERK1/2 phosphorylation was observed (Fig. 7B,C, third panels from above), indicating that this event is independent of MEK1/2 activity.

ERK1/2 is believed to be constitutively bound to MEK1/2 in the cytoplasm and activation of MEK1/2 not only phosphorylates ERK1/2 but also releases ERK1/2 from MEK1/2 so it can translocate to the nucleus. This could imply that MEK1/2-independent ERK1/2 phosphorylation may activate ERK1/2 but could prevent its nuclear translocation. Therefore, to address this issue, we performed cytosol/nuclear fractionation of CHO$\alpha_V\beta_3$ cell (Fig. 7Da) and osteoclast (Fig. 7Db) lysates, and observed phosphorylated ERK1/2 nuclear translocation in cells attached to LM609 both in control conditions and in the presence of PD98059 or U0126, thus ruling out that $\alpha_V\beta_3$-mediated signalling could result only in partial ERK1/2 activation. To assess the efficacy of the inhibitors and the specificity of the MEK1/2-independent pathway, we treated CHO$\alpha_V\beta_3$ cells (not shown) and osteoclasts (Fig. 7E) with 20% FBS, which contains a variety of mitogens inducing the canonical MEK1/2-dependent ERK1/2 activation, and consistently observed MEK1/2 phosphorylation (Fig. 7E,) as well as ERK1/2 phosphorylation (Fig. 7E,) and nuclear translocation (Fig. 7E), which were all inhibited by the PD98059 and U0126.

Taken together, these results suggest that ERK1/2 activation by $\alpha_V\beta_3$ engagement is not downstream of the canonical Ras/Raf-1/MEK1/2-dependent signals.

Role of calcium

As the PKCα is a Ca^{2+}-dependent PKC family member, we next assessed the role of Ca^{2+} in PKCα redistribution and recruitment by $\alpha_V\beta_3$, and in ERK1/2 activation. Addition of 2 mM O,O′-bis(2-aminoethyl)ethyleneglycol-N,N,N′,N′-tetraacetic acid (EGTA) to chelate extracellular Ca^{2+} was without effect (not shown). In contrast, chelation of intracellular Ca^{2+} by incubation with 2 mM EGTA/50 μM BAPTA-AM prevented adhesion-dependent PKCα translocation from cytosol to membrane and/or Triton X-100-insoluble fraction (Fig. 8A,B upper panels), PKCα recruitment by engaged $\alpha_V\beta_3$ (Fig. 8A,B, lower left panels) and ERK1/2 phosphorylation (Fig. 8A,B, lower right panel) both in CHO$\alpha_V\beta_3$ cells (Fig. 8A) and in osteoclasts (Fig. 8B). It is therefore clear that all the effects of $\alpha_V\beta_3$ on PKCα and on ERK1/2 activation are Ras/Raf-1/MEK1/2 independent but Ca^{2+} sensitive.

Role of PKCα in ERK1/2 activation

We next evaluated pharmacologically the involvement of

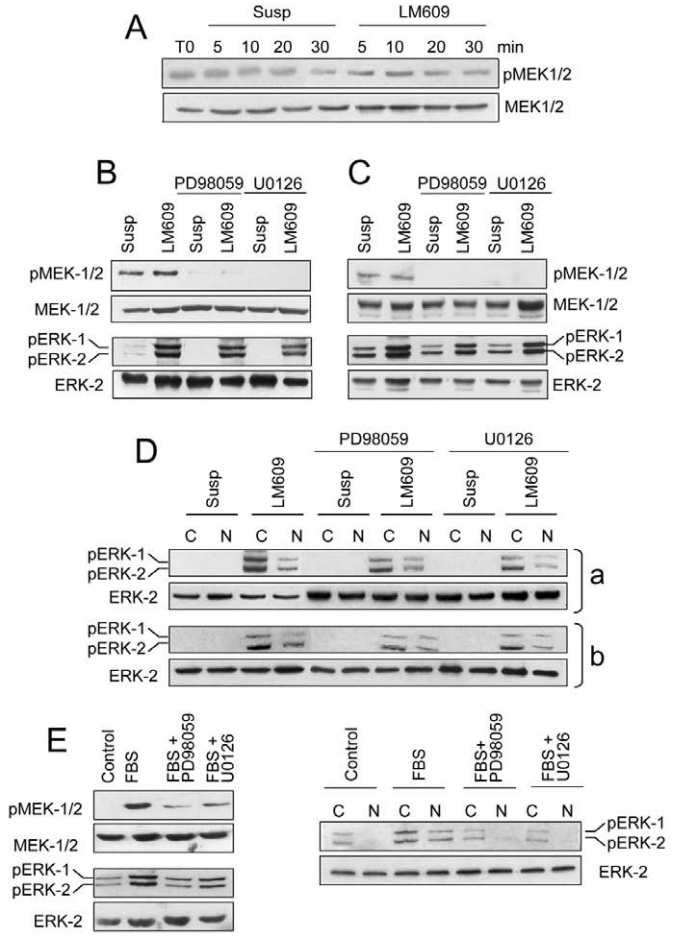

Fig. 7. MEK1/2 activation and effect of MEK1/2 inhibitors. (A) CHO$\alpha_V\beta_3$ cells were plated on immobilized LM609 substrate for the indicated times, lysed and total and phosphorylated MEK1/2 was determined. In the same gel, total and phosphorylated ERK1/2 were also detected (shown in Fig. 3C). (B) CHO$\alpha_V\beta_3$ cells and (C) osteoclasts were plated on immobilized LM609 substrate. Prior to plating, aliquots of cells were pretreated with the MEK1/2 inhibitors PD98059 (50 μM, 30 minutes) or U0126 (10 μM, 30 minutes). Lysates were subjected to western blot analysis and probed for detection of total and phosphorylated MEK1/2 and ERK1/2. (D)Lysates of (a) CHO$\alpha_V\beta_3$ cells and (b) osteoclasts treated as described above were also subjected to cytosol/nuclear fractionation and probed for detection of total and phosphorylated ERK1/2. (E) Osteoclasts cultured in standard conditions were starved in 1% FBS overnight, then stimulated with 20% FBS for 30 minutes. Total cell lysates (left panels) and cytosol/nuclear fractions (right panels) were then probed for detection of total and phosphorylated MEK1/2 and ERK1/2. Similar results were obtained in three independent experiments. Susp, cells in suspension; LM609, adhesion to LM609 for 30 minutes; C, cytosolic fraction; N, nuclear fraction.

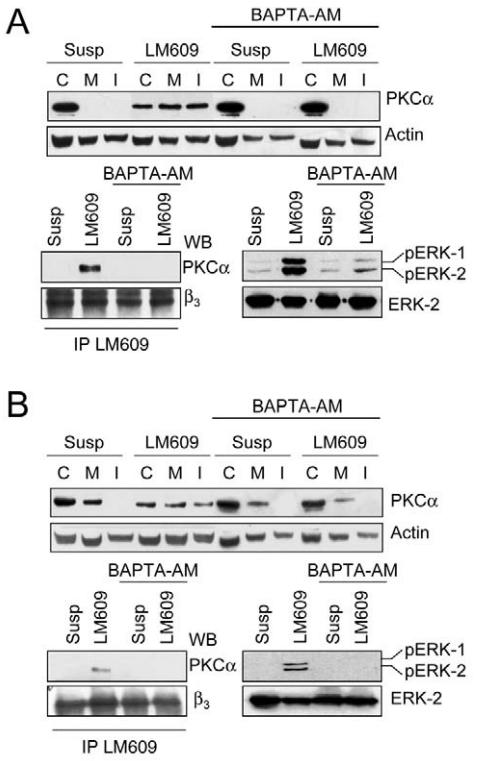

Fig. 8. The role of intracellular Ca^{2+}. (A) CHO$\alpha_V\beta_3$ cells and (B) osteoclasts were pretreated with the intracellular Ca^{2+} chelator BAPTA-AM (50 μM, 30 minutes) in the presence of 2 mM EGTA prior to adhesion to immobilized LM609 and protein fractionation (upper panels), immunoprecipitation with LM609 antibody (lower left panels) or western blotting (lower right panels). Lysates were then western blotted with the indicated antibodies. Similar results were obtained in three independent experiments. IP, immunoprecipitation; WB, western blot analysis; Susp, cells in suspension; LM609, adhesion to LM609 for 30 minutes.

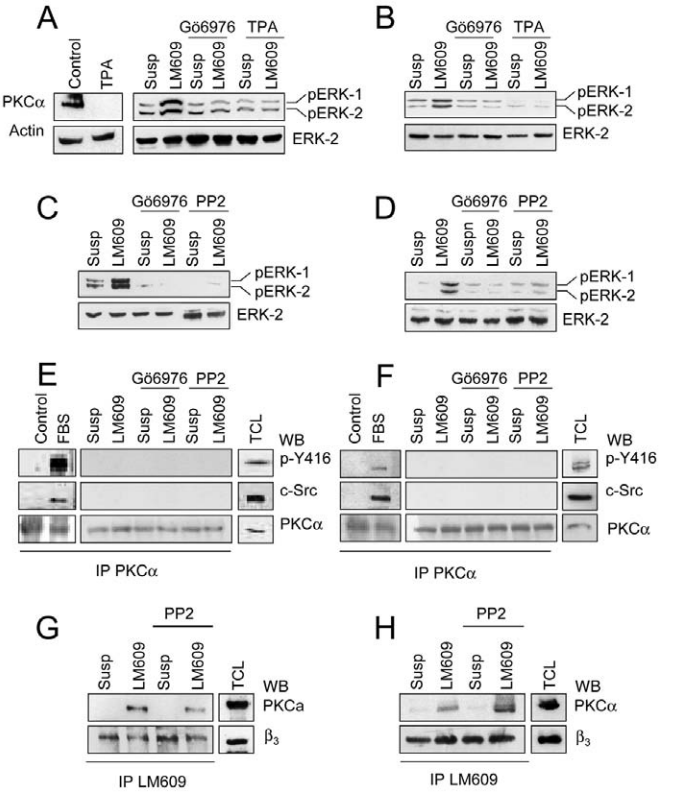

Fig. 9. PKCα-dependent ERK1/2 phosphorylation. (A) CHO$\alpha_V\beta_3$ cells and (B) osteoclast cultures were pretreated with the PKCα inhibitors (Gö6976, 6 nM for CHO$\alpha_V\beta_3$ and 2 μM for osteoclasts, 30 minutes; TPA 10^{-7} M, overnight) prior to plating on LM609 substrate and western blotting with the indicated antibodies. Left panels in A show down-regulation of PKCα upon overnight treatment with TPA. (C) CHO$\alpha_V\beta_3$3 cells and (D) osteoclast cultures were pretreated with the PKCα or c-Src (PP2, 50 μM, 30 minutes) inhibitors prior to plating on LM609 substrate and western blotting for total and phosphorylated ERKs. (E) CHO$\alpha_V\beta_3$ cells and (F) osteoclast cultures were pretreated with the PKCα or c-Src inhibitors prior to plating on LM609 substrate, followed by immunoprecipitation with anti-PKCα antibody and western blotting with the indicated antibodies to detect total and p-Y416 (activated) c-Src (diluted 1:1000). An aliquot of cells in standard culture conditions were serum-starved and then treated with 20% FBS for 30 minutes as positive control. (G) CHO$\alpha_V\beta_3$ cells and (H) osteoclast cultures were pretreated with the c-Src inhibitor prior to plating on LM609 substrate, followed by immunoprecipitation with LM609 antibody and western blotting with the indicated antibodies. Similar results were obtained in three independent experiments. IP, immunoprecipitation; WB, western blot analysis; Susp, cells in suspension; LM609, adhesion to LM609 for 30 minutes.

PKCα in $\alpha_V\beta_3$ integrin-mediated ERK1/2 phosphorylation. In Fig. 9A,B, the effect of the PKCα catalytic activity inhibitor, Gö6976, as well as that of the PKCα downregulation by long-term treatment with TPA (Fig. 9A left panels) are shown. Both inhibitors prevented ERK1/2 phosphorylation in CHO$\alpha_V\beta_3$ cells (Fig. 9A, right panels) and osteoclasts (Fig. 9B) upon adhesion to LM609.

Role of c-Src in ERK1/2 activation

c-Src is an important mediator of the $\alpha_V\beta_3$ signals (Sanjay et al., 2001). Therefore we investigated whether any interaction between this tyrosine kinase and PKCα was exhibited downstream of the integrin engagement. Similar lack of ERK1/2 activation was observed in CHO$\alpha_V\beta_3$ cells (Fig. 9C) and osteoclasts (Fig. 9D) treated with the c-Src inhibitor PP2. However, this effect appeared to be independent of physical interaction with PKCα. In fact, a complex with c-Src was not observed in cell lysates immunoprecipitated with PKCα antibody (Fig. 9E,F) in both cell types, which was, however, noticed in serum-starved cells treated with 20% FBS used as positive control. Moreover, in the presence of PP2, $\alpha_V\beta_3$ recruited PKCα upon adhesion to LM609 in a manner similar to untreated cells (Fig. 9G,H). Interestingly, as previously shown in Fig. 6B,C, Raf-1 activation was not downstream of c-Src, ruling out the involvement of the Ras/Raf-1/MEK1/2 pathway also in $\alpha_V\beta_3$ integrin-mediated, c-Src-dependent ERK1/2 phosphorylation.

Role of PKCα in $\alpha_V\beta_3$ integrin-mediated cell function

Finally, to assess the functional role of PKCα signalling induced by $\alpha_V\beta_3$ engagement in CHO$\alpha_V\beta_3$ cells and

osteoclasts, we performed adhesion experiments in the presence of PKCα inhibitor, Gö6976. We did not observe any change in the adhesion rate of CHO$\alpha_V\beta_3$ cells (Fig. 10A) or in the number of osteoclasts (Fig. 10B) attached to LM609, suggesting that activation of PKCα in our experimental conditions may affect events downstream of adhesion. Consistent with this hypothesis, we noted that migration of CHO$\alpha_V\beta_3$ cells (Fig. 10C) and osteoclasts (Fig. 10D), in Boyden chambers whose membranes were coated with LM609, was significantly reduced by the PKCα inhibitor. In contrast, the ability of CHO$\alpha_V\beta_3$ cells to penetrate through Matrigel, a reconstituted basement membrane recognized by several integrins, was not affected by Gö6976 (Fig. 10E). Notably, the osteoclast resorbing ability, evaluated by the pit assay, was significantly reduced (Fig. 10F) suggesting an important functional role in osteoclast activity. Finally, no effect of PKCα inhibitors were observed on cell survival (not shown).

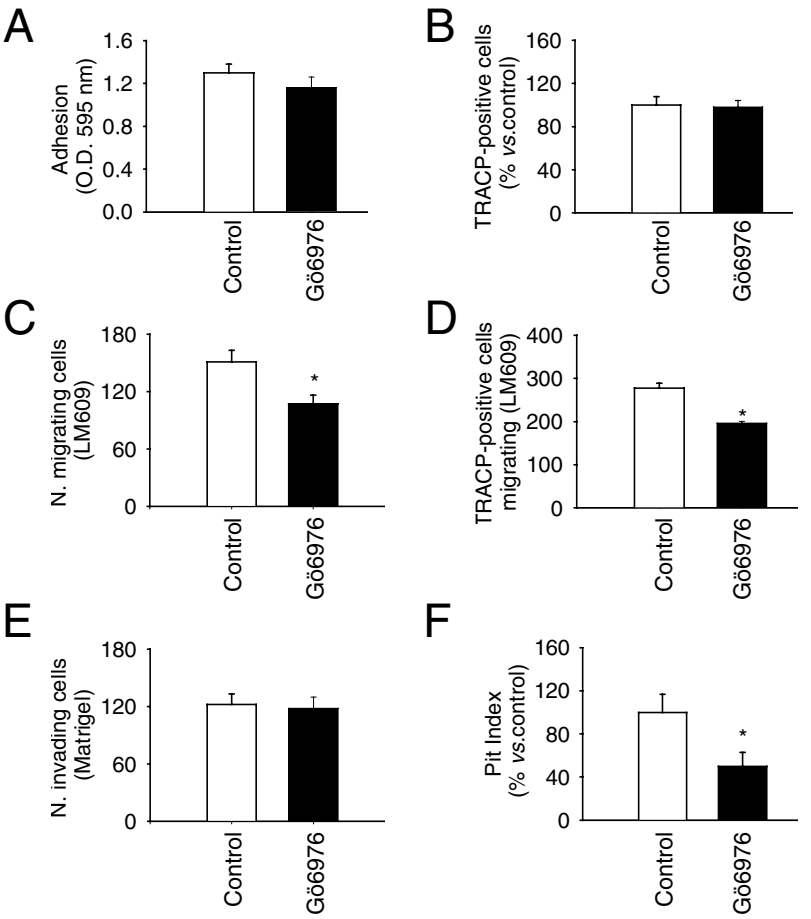

Fig. 10. Functional role of PKCα. CHO$\alpha_V\beta_3$ cells (left panels) and osteoclast cultures (right panels) were treated with Gö6976 as described in the Materials and Methods and investigated for (A,B) adhesion to LM609, (C,D) migration through LM609, (E) invasion through Matrigel and (F) bone resorption. Results are the mean ± s.e.m. from three independent experiments. *P<0.005. The times of each assay are as follows: (A,B) 30 minutes; (C,E) 4 hours; (D) 12 hours; (F) 48 hours.

Discussion

Despite the fact that the $\alpha_V\beta_3$ function is well known in osteoclasts and much information is available on its signalling mechanisms and interaction with membrane receptors relevant to the osteoclast activity (McHugh et al., 2000; Nakamura et al., 1999), the molecular machinery associated with its downstream effectors is still poorly understood (Duong et al., 2000). In this study, a role for the so-called classical (Ca^{2+}- and diacylglycerol-dependent) PKC isoform α has been elucidated. This serine/threonine kinase was found to be involved in $\alpha_V\beta_3$-mediated ERK1/2 activation in an intracellular Ca^{2+}-dependent manner, but independently of the adaptor protein Shc, of the Ras/Raf-1/MEK complex, and of the c-Src non-receptor tyrosine kinase signals.

In previous reports, the use of promiscuous substrates recognized by more than one integrin may have made it difficult to dissect the mechanisms associated with each specific matrix receptor (Arnaut et al., 2002). In our study, we used a highly specific monoclonal antibody, largely employed to activate the $\alpha_V\beta_3$ receptor (Bhattacharya et al., 2000; Murphy et al., 2003), and detected the downstream signals associated exclusively with this integrin. This is indicated by the fact that in CHO cell lines, only the clonal cells carrying the $\alpha_V\beta_3$ receptor and not the parental cells, expressing the α_V but not the β_3 subunit, could adhere to the LM609 antibody. Adhesion to this substrate triggered PKCα translocation, i.e. activation, and subsequent ERK1/2 phosphorylation in CHO$\alpha_V\beta_3$ cells and also in osteoclasts, which are known to express high copy numbers of the $\alpha_V\beta_3$ receptor (Duong et al., 2000; Villanova et al., 1999; Helfrich et al., 1996).

$\alpha_V\beta_3$ ligation-dependent ERK1/2 phosphorylation was prevented by the PKCα-specific inhibitor Gö6976, and by downregulation of PKCα by long-term treatment with TPA, demonstrating that it occurs as a result of activation of this PKC isoform. PKCα inhibition also had functional consequences, causing reduction in migration ability and, in the case of osteoclasts, also reduction in bone resorption. These observations suggest that an important role of PKCα activation downstream of $\alpha_V\beta_3$ engagement could be with cell motility, the impairment of which could also affect the ability of osteoclasts to resorb bone. No changes in survival rate were observed when cells were treated with Gö6976 (not shown), and this inhibitor did not alter the ability of cells to interact with the LM609 substrate, clearly indicating that the PKCα involvement occurs mainly in post-adhesion events.

It is interesting to note that $\alpha_V\beta_3$ integrin-mediated PKCα translocation occurred to the Triton-X-insoluble fraction, particularly in osteoclasts, where similar levels of the enzyme were instead found in the Triton-X-soluble, membrane fraction, irrespective of $\alpha_V\beta_3$ engagement. This compartment is believed to consist of membrane microdomains, denominated lipid rafts, that are enriched in cholesterol and glycosphingolipids, implicated in several processes, including signal transduction, endocytosis, membrane trafficking,

cytoskeletal reorganization and pathogen entry (Munro, 2003; Pike, 2004). $\alpha_V\beta_3$ integrin may be accumulated in rafts (Triantafilou and Triantafilou, 2003), and its ligand-induced activation is enhanced by glycosyl phosphatidylinositol anchor (McDonald et al., 2004). Lipid raft integrity is required for receptor-mediated actin cytoskeleton reorganization and PKCα translocation (Becart et al., 2003) and the raft fraction is assumed to be important for the Ca^{2+} signalling and the Ca^{2+}-dependent association of classical PKC to these microdomains (Orito et al., 2001). It is, therefore, possible that this fraction may play an important role in the Ca^{2+}-dependent PKCα signalling induced by ligand-dependent $\alpha_V\beta_3$ activation.

Interestingly, within the MAPK family, only ERK1/2 were found to be activated by signals triggered by $\alpha_V\beta_3$ ligation. Neither p38 nor JNK were altered by adhesion to LM609, and ERK1/2 phosphorylation was triggered in response to $\alpha_V\beta_3$-mediated adhesion not only in a PKCα-, but also in a Ca^{2+}- and c-Src-dependent manner.

$[Ca^{2+}]_i$ appears to be central to the $\alpha_V\beta_3$ signal transduction pathway. It has been previously demonstrated that adhesion of osteoclasts to $\alpha_V\beta_3$ substrates induces intracellular Ca^{2+} mobilization, which is believed to be an important signal for cytoskeletal remodelling (Duong et al., 2000). Cytosolic Ca^{2+} acts at, at least, three levels: PKCα (this study), PYK2 (Lev et al., 1995) and gelsolin (Robinson et al., 2000). These three pathways are regulated in a Ca^{2+}-dependent fashion and are implicated in different downstream events associated with $\alpha_V\beta_3$-mediated signals. PYK2 appears to recruit c-Src to the adhesion sites and trigger c-Src-dependent c-Cbl phosphorylation which has been suggested to cause ubiquitination and proteasome degradation of the podosome molecular complex (Sanjay et al., 2001). These events may be highly relevant for podosome assembly/disassembly cycles which make these adhesions highly dynamic. Another Ca^{2+}-sensitive component of podosomes is the microfilament-severing protein gelsolin (Akisaka et al., 2001). This protein, which is associated with phosphatidylinositol bisphosphate in the membrane, is released from it upon receptor-mediated lipid breakdown, and is activated in a Ca^{2+}-dependent manner to severe pre-existing microfilaments and nucleate new microfilaments for cytoskeletal remodelling (Wang et al., 2003). Results from our study also include PKCα in this scenario. Its $\alpha_V\beta_3$-dependent subcellular redistribution and recruitment in a complex with $\alpha_V\beta_3$ integrin is, not surprisingly, largely dependent on cytosolic Ca^{2+} concentration and is prevented by the intracellular Ca^{2+} chelator BAPTA. PKCα is member of the classical, Ca^{2+} and diacylglycerol dependent, PKCs and its activation by cytosolic Ca^{2+} was expected. Miranti et al. (Miranti et al., 1999) had previously suggested that integrin-associated PKC signal was triggered by phospholipase C (PLC)γ1, an event found not to occur in our study (not shown). However, we found that phosphoinositide 3-kinase, which is also involved in integrin-induced signalling (Duong et al., 2000), is not implicated in PKCα recruitment by the $\alpha_V\beta_3$ receptor, or in ERK1/2 activation (not shown); the upstream regulators of this signal, therefore, remain to be elucidated.

Cytosolic Ca^{2+} chelation by BAPTA inhibited ERK1/2 phosphorylation upon adhesion of cells to LM609. Consistent with this result, inhibition of PKCα by the specific inhibitor Gö6976, or by long-term exposure to TPA, also prevented ERK1/2 phosphorylation. Analogous inhibition was observed upon pre-treatment of cells with the c-Src kinase inhibitor, PP2, but this mechanism appeared to be independent of PKCα, as the two kinases were not found to be associated in a molecular complex upon engagement of $\alpha_V\beta_3$ integrin, neither was the formation of the $\alpha_V\beta_3$/PKCα complex prevented by PP2.

PKCα and c-Src downstream signals of ERK1/2 phosphorylation remain to be established. Surprisingly, we could not observe Shc engagement in a complex with $\alpha_V\beta_3$ integrin, or its phosphorylation or subcellular redistribution. Therefore, at variance with previous results (Giancotti and Ruoslahti, 1999; Hood and Cheresh, 2002), in our experimental conditions, Shc appears not to be involved in the $\alpha_V\beta_3$ activation of ERK1/2. However, we did observe recruitment of Grb2 into a complex with the integrin upon adhesion of cells to LM609. In other signalling pathways, Grb2 has been shown to establish direct molecular interactions with FAK or PYK2, independent of Shc (Schlaepfer and Hunter, 1996). Most intriguing, however, is the observation that downstream of Grb2, neither Ras, Raf-1 nor MEK1/2 were involved in ERK1/2 activation. There are only a few examples in the literature suggesting alternative pathways for ERK1/2 involving classical PKCs that, at variance with our findings, co-exist with the typical Ras/Raf-1/MEK1/2 cascade (Grammer and Blenis, 1997). These pathways are known to regulate the prolonged activation of ERK1/2, but their specific components remain to be elucidated.

Similar independence of MEK1/2 was observed in the c-Src pathway leading to ERK1/2 phosphorylation, suggested by the lack of c-Src-induced MEK1/2 tyrosine phosphorylation. Therefore, it appears that PKCα and c-Src converge on ERK1/2 in response to $\alpha_V\beta_3$ ligation, although they do not seem to interact in the same complex. In T-cells, Niu et al. (Niu et al., 2003) have shown a link between a member of the c-Src family (Lck) and PKC in response to activation of a subset of integrins (β_1) requiring the CD45 receptor tyrosine kinase. However, this interaction leads to Shc activation, an event not observed in our experimental conditions.

In conclusion, our study suggests that PKCα is central to $\alpha_V\beta_3$-mediated intracellular signalling inducing ERK1/2 activation by a novel pathway, and that it regulates events downstream of adhesion, including cell migration and, in the case of osteoclasts, bone resorption.

This work was supported by the Telethon grant E.0831, the Fondo per gli Investimenti per la Ricerca di Base (FIRB) grant RBAU01X3NH, the Associazione Italiana per la Ricerca sul Cancro (AIRC), the Agenzia Spaziale Italiana (ASI) grant I/R/108/00 and EC grants METABRE (contract no. LSHM-CT-2003-503049) and OSTEOGENE (contract no. LSHM-CT-2003-502941) to A.T. The excellent technical support of Luigi Pellegrino and Rita Di Massimo is gratefully acknowledged.

References

Akisaka, T., Yoshida, H., Inoue, S. and Shimizu, K. (2001). Organization of cytoskeletal F-actin, G-actin, and gelsolin in the adhesion structures in cultured osteoclasts. *J. Bone Miner. Res.* **16**, 1248-1255.

Aplin, A. E., Howe, A., Alahari, S. K. and Juliano, R. L. (1998). Signal transduction and signal modulation by cell adhesion receptors: the role of integrins, cadherins, immunoglobulin-cell-adhesion molecules, and selectins. *Pharmacol. Rev.* **50**, 197-263.

Arnaout, M. A., Goodman, S. L. and Xiong, J. P. (2002). Coming to grips with integrin binding to ligands. *Curr. Opin. Cell Biol.* **14**, 641-651.

Becart, S., Setterblad, N., Ostrand-Rosenberg, S., Ono, S. J., Charror, D. and Mooney, N. (2003). Intracytoplasmic domains of MCH class II molecules are essential for lipid-raft-dependent signalling. *J. Cell Sci.* **116**, 2565-2575.

Bhattacharya, S., Ying, X., Fu, C., Patel, R., Kuebler, W., Greenberg, S. and Bhattacharya, J. (2000). α(v)β(3) integrin induces tyrosine phosphorylation-dependent Ca(2+) influx in pulmonary endothelial cells. *Circ. Res.* **86**, 456-462.

Boyle, W. J., Simonet, W. S. and Lacey, D. L. (2003). Osteoclast differentiation and activation. *Nature* **423**, 337-342.

Caselli, G. F., Mantovanini, M., Gandolfi, C. A., Allegretti, M., Fiorentino, S., Pellegrini, L., Melillo, G., Bertini, R., Sabbatini, W., Anacardio, R. et al. (1997). Tartronates: a new generation of drugs affecting bone metabolism. *J. Bone Miner. Res.* **12**, 972-981.

Chellaiah, M., Kizer, N., Silva, M., Alvarez, U., Kwiatkowski, D. and Hruska, K. A. (2000). Gelsolin deficiency blocks podosome assembly and produces increased bone mass and strength. *J. Cell Biol.* **148**, 665-678.

Chen, Q., Kinch, M. S., Lin, T. H., Burridge, K. and Juliano, R. L. (1994). Integrin-mediated cell adhesion activates mitogen-activated protein kinases. *J. Biol. Chem.* **269**, 26602-26605.

Chen, W. T. (1990). Transmembrane interactions at cell adhesion and invasion sites. *Cell. Differ. Dev.* **32**, 329-336.

David, J. P., Neff, L., Chen, Y., Rincon, M., Horne, W. C. and Baron, R. (1998). A new method to isolate large numbers of rabbit osteoclasts and osteoclast-like cells: application to the characterization of serum response element binding proteins during osteoclast differentiation. *J. Bone Miner. Res.* **13**, 1730-1738.

Destaing, O., Saltel, F., Géminard, J. C., Jurdic, P. and Bard, F. (2003). Podosomes display actin turnover and dynamic self-organization in osteoclasts expressing actin-green fluorescent protein. *Mol. Biol. Cell* **14**, 407-416.

Duong, L. T., Lakkakorpi, P. T., Nakamura, I. and Rodan, G. A. (2000). Integrins and signalling in osteoclast function. *Matrix Biol.* **19**, 97-105.

Foschi, M., Chari, S., Dunn, M. J. and Sorokin, A. (1997). Biphasic activation of $p21^{ras}$ by endothelin-1 sequentially activates the ERK cascade and phosphatidylinositol 3-kinase. *EMBO J.* **16**, 6439-6451.

Giancotti, F. G. and Ruoslahti, E. (1999). Integrin signalling. *Science* **285**, 1028-1032.

Grammer, T. C. and Blenis, J. (1997). Evidence for MEK-independent pathways regulating the prolonged activation of the ERK-MAP kinsases. *Oncogene* **14**, 1635-1642.

Guo, W. and Giancotti, F. G. (2004). Integrin signalling during tumour progression. *Nat. Rev. Mol. Cell. Biol.* **5**, 816-826.

Helfrich, M. H., Nesbitt, S. A., Lakkakorpi, P. T., Barnes, M. J., Bodary, S. C., Shankar, G., Mason, W. T., Mendrick, D. L., Vaananen, H. K. and Horton, M. A. (1996). β1 integrins and osteoclast function: involvement in collagen recognition and bone resorption. *Bone* **19**, 317-328.

Hofmann, J. (1997). The potential for isoenzyme selective modulation of protein kinase C. *FASEB J.* **11**, 649-669.

Hood, J. D. and Cheresh, D. A. (2002). Role of integrins in cell invasion and migration. *Nat. Rev. Cancer* **2**, 91-100.

Housey, G. M., Johnson, M. D., Hsiao, W. L., O'Brian, C. A. and Weinstein, I. B. (1988). Structural and functional studies of protein kinase C. *Adv. Exp. Med. Biol.* **234**, 127-140.

Jin, H. and Varner, J. (2004). Integrins, roles in cancer development and as treatment targets. *Br. J. Cancer* **90**, 561-565.

Kelly, T., Mueller, S. C., Yeh, Y. and Chen, W. T. (1994). Invadopodia promote proteolysis of a wide variety of extracellular matrix proteins. *J. Cell. Physiol.* **158**, 299-308.

Kim, H. H., Chung, W. J., Lee, S. W., Chung, P. J., You, J. W., Kwon, H. J., Tanaka, S. and Lee, Z. H. (2003). Association of sustained ERK activity with integrin β3 induction during receptor activator of nuclear factor kappaB ligand (RANKL)-directed osteoclast differentiation. *Exp. Cell Res.* **289**, 368-377.

Kumar, C. C. (2003). Integrin αVβ3 as a therapeutic target for blocking tumor-induced angiogenesis. *Curr. Drug Targets* **4**, 123-131.

Lev, S., Moreno, H., Martinez, R., Canoll, P., Peles, E., Musacchio, J. M., Plowman, G. D., Rudy, B. and Schlessinger, J. (1995). Protein tyrosine kinase PYK2 involved in Ca^{2+}-induced regulation of ion channel and MAPkinase function. *Nature* **376**, 737-745.

Linder, S. and Aepfelbacher, M. (2003). Podosomes: adhesion hot-spots of invasive cells. *Trends Cell Biol.* **13**, 376-385.

Malgaroli, A., Meldolesi, J., Zambonin Zallone, A. and Teti, A. (1989). Control of cytosolic free calcium in rat and chicken osteoclasts. The role of extracellular calcium and calcitonin. *J. Biol. Chem.* **264**, 14342-14347.

Marchisio, P. C., Cirillo, D., Naldini, L., Primavera, M. V., Teti, A. and Zambonin-Zallone, A. (1984). Cell-substratum interaction of cultured avian osteoclasts is mediated by specific adhesion structures. *J. Cell Biol.* **99**, 1696-1705.

McDonald, J. F., Zheleznyak, A. and Frazier, W. A. (2004). Cholesterol-independent interactions with CD47 enhance αVβ3 avidity. *J. Biol. Chem.* **279**, 17301-17311.

McHugh, K. P., Hodivala-Dilke, K., Zheng, M. H., Namba, N., Lam, J., Novack, D., Feng, X., Ross, F. P., Hynes, R. O. and Teitelbaum, S. L. (2000). Mice lacking β3 integrins are osteosclerotic because of dysfunctional osteoclasts. *J. Clin. Invest.* **105**, 433-440.

McNiven, M. A., Baldassarre, M. and Buccione, R. (2004). The role of dynamin in the assembly and function of podosomes and invadopodia. *Front. Biosci.* **9**, 1944-1953.

Miranti, C. K., Ohno, S. and Brugge, J. S. (1999). Protein kinase C regulates integrin-induced activation of the extracellular regulated kinase pathway upstream of Shc. *J. Biol. Chem.* **274**, 10571-10581.

Miyauchi, A., Hruska, K. A., Greenfield, E. M., Randall, D., Alvarez, J., Barattolo, R., Colucci, S., Zambonin Zallone, A., Teitelbaum, S. L. and Teti, A. (1990). Osteoclast cytosolic calcium, regulated by voltage operated calcium channels and extracellular calcium, controls podosome assembly and bone resorption. *J. Cell Biol.* **111**, 2543-2552.

Munro, S. (2003). Lipid rafts: elusive or illusive? *Cell* **115**, 377-388.

Murphy, J. F., Steele, C., Belton, O. and Fitzgerald, D. J. (2003). Induction of cyclooxygenase-1 and -2 modulates angiogenic responses to engagement of αVβ3. *Br. J. Haematol.* **121**, 157-164.

Naik, M. U., Mousa, S. A., Parkos, C. A. and Naik, U. P. (2003). JAM-1 and αVβ3 is required for the angiogenic action of bFGF: dissociation of the JAM-1 and αVβ3 complex. *Blood* **102**, 2108-2114.

Nakamura, I., Pilkington, M. F., Lakkakorpi, P. T., Lipfert, L., Sims, S. M., Dixon, S. J., Rodan, G. A. and Duong, L. T. (1999). Role of αVβ3 integrin in osteoclast migration and formation of the sealing zone. *J. Cell Sci.* **112**, 3985-3993.

Nakamura, H., Hirata, A., Tsuji, T. and Yamamoto, T. (2003). Role of osteoclast extracellular signal-regulated kinase (ERK) in cell survival and maintenance of cell polarity. *J. Bone Min. Res.* **18**, 1198-1205.

Naro, F., Perez, M., Migliaccio, S., Galson, D. L., Orcel, P., Teti, A. and Goldring, S. R. (1998). Phospholipase D- and protein kinase C isenzyme-dependent signal transduction pathway activated by the calcitonin receptor. *Endocrinology* **139**, 3241-3248.

Nemeth, J. A., Cher, M. L., Zhou, Z., Mullins, C., Bhagat, S. and Trikha, M. (2003). Inhibition of α(v)β3 integrin reduces angiogenesis, bone turnover, and tumor cell proliferation in experimental prostate cancer bone metastases. *Clin. Exp. Metastasis* **20**, 413-420.

Ni, C. W., Wang, D. L., Lien, S. C., Cheng, J. J., Chao, Y. J. and Hsieh, H. J. (2003). Activation of PKC-ε and ERK1/2 participates in shear-induced endothelial MCP-1 expression that is repressed by nitric oxide. *J. Cell. Physiol.* **195**, 428-434.

Niu, S., Xie, H. and Marcantonio, E. E. (2003). Integrin-mediated tyrosine phosphorylation of Shc in T cells is regulated by protein kinase C-dependent phosphorylation of Lck. *Mol. Biol. Cell* **14**, 349-360.

Orito, A., Kumanogoh, H., Yasaka, K., Sokawa, J., Hidaka, H., Sokawa, Y. and Maekawa, S. (2001). Calcium-dependent association of annexin VI, protein kinase C α, and neurocalcin α on the raft fraction derived from the synaptic plasma membrane of rat brain. *J. Neurosci. Res.* **64**, 235-241.

Pfaff, M. and Jurdic, P. (2001). Podosomes in osteoclast-like cells: structural analysis and cooperative roles of paxillin, proline-rich tyrosine kinase 2 (Pyk2) and integrin αVβ3. *J. Cell Sci.* **114**, 2775-2786.

Pike, L. J. (2004). Lipid rafts: heterogeneity on the high seas. *Biochem. J.* **378**, 281-292.

Pintus, G., Tadolini, B., Posadino, A. M., Sanna, B., Debidda, M., Carru, C., Deiana, L. and Ventura, C. (2003). PKC/Raf/MEK/ERK signalling pathway modulates native-LDL-induced E2F-1 gene expression and endothelial cell proliferation. *Cardiovasc. Res.* **59**, 934-944.

Robinson, R. C., Meijillano, M., Le, V. P., Burtnick, L. D., Yin, H. L. and Choe, S. (2000). Domain movement in gelsolin: a calcium-activated switch. *Science* **286**, 1939-1942.

Ross, F. P., Chappel, J., Alvarez, J. I., Sander, D., Butler, W. T., Farach-Carson, M. C., Mintz, K. A., Robey, P. G., Teitelbaum, S. L. and Cheresh, D. A. (1993). Interactions between the bone matrix proteins osteopontin and bone sialoprotein and the osteoclast integrin αVβ3 potentiate bone resorption. *J. Biol. Chem.* **152**, 181-195.

Saltel, F., Destaing, O., Bard, F., Eichert, D. and Jurdic, P. (2004). Apatite-

mediated actin dynamics in resorbing osteoclasts. *Mol. Biol. Cell* **15**, 5231-5241.

Sanjay, A., Houghton, A., Neff, L., DiDomenico, E., Bardelay, C., Antoine, E., Levy, J., Gailit, J., Bowtell, D., Horne, W. C. et al. (2001). Cbl associates with Pyk2 and Src to regulate Src kinase activity, αVβ3 integrin mediated signalling, cell adhesion, and osteoclast motility. *J. Cell Biol.* **152**, 181-195.

Schlaepfer, D. D. and Hunter, T. (1996). Evidence for in vivo phosphorylation of the Grb2 SH2-domain binding site on focal adhesion kinase by Src-family protein-tyrosine kinases. *Mol. Cell. Biol.* **16**, 5623-5633.

Schlaepfer, D. D., Hanks, S. K., Hunter, T. and van der Geer, P. (1994). Integrin-mediated signal transduction linked to Ras pathway by Grb2 binding to focal adhesion kinase. *Nature* **372**, 786-791.

Tanaka, S., Nakamura, I., Inoue, J., Oda, H. and Nakamura, K. (2003). Signal transduction pathways regulating osteoclast differentiation and function. *J. Bone Miner. Metab.* **21**, 123-133.

Teitelbaum, S. L. (2000). Bone resoprtion by osteoclasts. *Science* **289**, 1501-1504.

Teti, A., Blair, H. C., Schlesinger, P., Grano, M., Zambonin Zallone, A., Kahn, A. J., Teitelbaum, S. L. and Hruska, K. A. (1989). Extracellular protons acidify osteoclasts, reduce cytosolic calcium and promote expression of cell-matrix attachment structures. *J. Clin. Invest.* **84**, 773-780.

Teti, A., Marchisio, P. C. and Zambonin Zallone, A. (1991). Clear zone in osteoclast function: role of podosomes in regulation of bone resorbing activity. *Am. J. Physiol.* **261**, C1-C7.

Teti, A., Paniccia, R. and Goldring, S. R. (1995). Calcitonin increases cytosolic free calcium concentration via capacitative calcium influx. *J. Biol. Chem.* **270**, 16666-16670.

Teti, A., Migliaccio, S. and Baron, R. (2002). The role of the αVβ3 integrin in the development of osteolytic bone metastases: a pharmacological target for alternative therapy. *Calcif. Tissue Int.* **71**, 293-299.

Triantafilou, K. and Triantafilou, M. (2003). Lipid raft microdomains: key sites for Coxsackievirus A9 infectious cycle. *Virology* **317**, 128-135.

Varner, J. A. and Cheresh, D. A. (1996). Integrins and cancer. *Curr. Opin. Cell Biol.* **8**, 724-730.

Villanova, I., Townsend, P. A., Uhlmann, E., Knolle, J., Peyman, A., Amling, M., Baron, R., Horton, M. A. and Teti, A. (1999). Oligodeoxynucleotide targeted to the αV gene inhibits αV integrin synthesis, impairs osteoclast function and activates intracellular signals to apoptosis. *J. Bone Miner. Res.* **14**, 1867-1879.

Wang, Q., Xie, Y., Du, Q. S., Wu, X. J., Feng, X., Mei, L., McDonald, J. M. and Xiong, W. C. (2003). Regulation of the formation of osteoclastic actin rings by proline rich tyrosine kinase 2 interacting with gelsolin. *J. Cell Biol.* **160**, 565-575.

Zhang, Z., Neff, L., Bothwell, A. L., Baron, R. and Horne, W. C. (2002). Calcitonin induces dephosphorylation of Pyk2 and phopshorylation of focal adhesion kinase in osteoclasts. *Bone* **31**, 359-365.